nature chemical biology

Rapid selection of cyclic peptides that reduce α-synuclein toxicity in yeast and animal models

Joshua A Kritzer[1], Shusei Hamamichi[2], J Michael McCaffery[3], Sandro Santagata[1,4], Todd A Naumann[5], Kim A Caldwell[2], Guy A Caldwell[2] & Susan Lindquist[1,6]

Phage display has demonstrated the utility of cyclic peptides as general protein ligands but cannot access proteins inside eukaryotic cells. Expanding a new chemical genetics tool, we describe the first expressed library of head-to-tail cyclic peptides in yeast (*Saccharomyces cerevisiae*). We applied the library to selections in a yeast model of α-synuclein toxicity that recapitulates much of the cellular pathology of Parkinson's disease. From a pool of 5 million transformants, we isolated two related cyclic peptide constructs that specifically reduced the toxicity of human α-synuclein. These expressed cyclic peptide constructs also prevented dopaminergic neuron loss in an established *Caenorhabditis elegans* Parkinson's model. This work highlights the speed and efficiency of using libraries of expressed cyclic peptides for forward chemical genetics in cellular models of human disease.

Cyclic peptides (CPs) and their derivatives are potent bioactive compounds and represent an underexplored, natural-product-like chemical space[1,2]. Phage and RNA display have made it possible to screen large libraries of CPs, cyclized through disulfide bonds or other side chain linkages, to identify high-affinity ligands for nearly any *in vitro* target[3,4]. By contrast, there are as yet few methods for directly screening large libraries of CPs inside eukaryotic cells. Such methods would provide several advantages over *in vitro* techniques, ensuring that hits are nontoxic, can bind their target(s) in the appropriate cellular environment, are not rapidly degraded by cellular proteases and possess at least enough selectivity to function in living cells. In addition, *in vivo* methods would enable phenotypic selection of CPs, providing a less expensive alternative to traditional high-throughput screening with a greater chance of identifying effectors with nontraditional modes of action, such as inhibition of protein-protein interactions.

Recent reports have described a robust method, named SICLOPPS (split-intein-mediated circular ligation of proteins and peptides, **Fig. 1a**)[5–7], of generating libraries of head-to-tail CPs *in vivo* using a single genetic construct. This construct uses a split intein arranged so that a linker region is post-translationally spliced out as a CP; the linker can be as small as four amino acids or as large as a whole protein[5,8]. SICLOPPS-based CP libraries present an opportunity for rapid forward and reverse chemical genetics using *in vivo* selections[7]. Previous work has interfaced expressed CP libraries with bacterial two-hybrid selections, a versatile strategy for reverse chemical genetics[7,9]. Phenotypic screening of CP libraries was also performed in bacteria[10,11]. Despite these successes, there has so far been only one reported attempt to adapt SICLOPPS libraries to a eukaryotic system. A retroviral CP library was applied to a selection for inhibitors of interleukin-4 signaling in human B cells, yielding roughly a dozen CP pentamers with varying activity but no sequence consensus[12]. The general utility of this library was hampered by its low actual diversity (2.7×10^5 members), a lack of quantitative quality assessment and the several weeks required just to perform an initial round of selection. Building on these earlier studies, we sought to apply expressed CP libraries to eukaryotic cells and perform phenotypic selections in cellular models of human disease in a rapid, efficient and generally applicable manner.

We and others have demonstrated that, because protein misfolding often affects highly conserved biological pathways, complex diseases such as Parkinson's disease can be modeled in simple organisms such as yeast[13–18]. The human protein α-synuclein (α-syn) has been linked to Parkinson's disease by genetic evidence and its prominence in the Parkinson's disease–associated intracellular aggregates known as Lewy bodies[19–21]. Alpha-syn is a small, lipid-binding protein that is prone to misfolding and aggregation, and in the yeast *S. cerevisiae* expression of human α-syn over a threshold level leads to endoplasmic reticulum stress, disruption of endoplasmic reticulum–Golgi vesicle trafficking, accumulation of lipid droplets, mitochondrial dysfunction, and, ultimately, cell death[16–18]. This cellular pathology mirrors many aspects of dysfunction seen in neurons and glia of individuals with Parkinson's disease and other synucleinopathies[21]. Genetic screening using our yeast synucleinopathy model has yielded suppressors of α-syn toxicity that are also effective in neuronal models[17,18,22]. Moreover, genetic analyses in these models have directly linked α-syn toxicity to the function of *PARK9*, a gene whose mutations lead

[1]Whitehead Institute for Biomedical Research, Cambridge Massachusetts, USA. [2]Department of Biological Sciences, University of Alabama, Tuscaloosa, Alabama, USA. [3]Integrated Imaging Center and Department of Biology, Johns Hopkins University, Baltimore, Maryland, USA. [4]Department of Pathology, Brigham and Women's Hospital and Harvard Medical School, Boston, Massachusetts, USA. [5]Department of Chemistry, The Pennsylvania State University, University Park, Pennsylvania, USA. [6]Howard Hughes Medical Institute, Department of Biology, Massachusetts Institute of Technology, Cambridge Massachusetts, USA. Correspondence should be addressed to S.L. (lindquist_admin@wi.mit.edu).

Received 31 March; accepted 8 May; published online 13 July 2009; doi:10.1038/nchembio.193

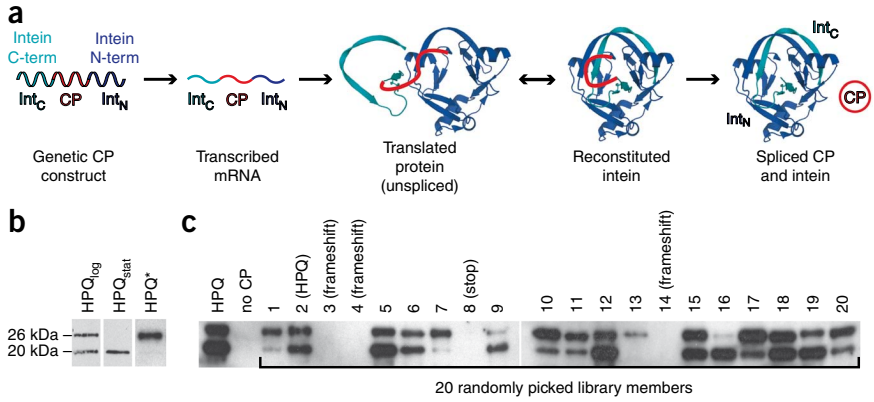

Figure 1 A cyclic peptide library that expresses and processes in yeast. (**a**) The SICLOPPS construct encodes a single protein that yields a CP after post-translational splicing[5]. The *dnaE* intein C-terminal domain is encoded first, followed by the linker to be cyclized, the intein N-terminal domain, and finally a chitin-binding-domain affinity tag (not shown). Graphic was generated using the crystal structure of the post-splicing form of the *Synechocystis* sp. PCC6803 *dnaE* intein, PBD ID 1ZD7 (ref. 26). (**b**) Western blots for the affinity tag quantify the expression and processing of the split intein construct. Log-phase yeast cultures expressing the control HPQ construct (HPQ$_{log}$) showed robust expression and ~50% distribution between the unprocessed 26-kDa construct and the processed 20 kDa byproduct. Yeast blotted at stationary phase (HPQ$_{stat}$) showed complete processing, whereas an HPQ variant with intein-disabling T69A H72A mutations (HPQ*) showed no processed byproduct in log phase. (**c**) Blots of log-phase cultures of yeast transformed with 20 randomly picked library members demonstrated that roughly 70% of the library encoded novel CP constructs that expressed and processed in yeast.

to an early-onset form of Parkinson's disease but which otherwise had no known connection to α-syn[22,23]. Thus, cellular models have been critical to our understanding of α-syn and its role in the selective degeneration of dopaminergic neurons in Parkinson's disease. However, despite these and other intensive efforts, there remains a paucity of proven pharmacological targets for Parkinson's disease and other synucleinopathies.

Taking advantage of our established yeast synucleinopathy model, we constructed the first yeast-compatible CP library and used rapid phenotypic selections to isolate CPs that specifically reduce α-syn toxicity. Further, we identified the CP motif responsible for activity and demonstrated that the selected CPs significantly reduce dopaminergic neuron loss in a *C. elegans* Parkinson's disease model. These advances establish *in vivo* CP selections as a tool immediately useful to a broad range of biologists.

RESULTS

The SICLOPPS construct expresses and splices in yeast

We expressed a SICLOPPS construct using a high-copy 2μ plasmid in *S. cerevisiae* under a constitutive *PGK* promoter. Lysates from log-phase and stationary-phase cultures were blotted using an antibody to a C-terminal tag (**Fig. 1b**), which revealed the expression level and processing status of the split intein construct[8]. The log-phase cultures showed approximately equal amounts of 26-kDa and 20-kDa proteins, which are the expected sizes of the unprocessed and processed constructs, respectively. Cultures harvested in stationary phase showed only the 20-kDa band, corresponding to a processed form of the construct that has undergone either complete splicing or hydrolysis. These findings are consistent with a splicing reaction that is somewhat slower than the rate of log-phase *PGK*-driven protein synthesis.

An intein-disabled version of the gene was constructed by mutating the residues corresponding to T69 and H72 of the *dnaE* split intein to alanine. Previous work has established that these mutations, which reside in conserved block B, permit association of the two halves of the split intein but prohibit processing at the extein/N-intein junction. This blocks the first obligatory step in the accepted splicing mechanism[24–26]. When a T69A H72A mutant of the construct was expressed in yeast, only the full-length, unprocessed form was detected (**Fig. 1b**). Thus, the lower, 20-kDa band indeed represents the expected product of intein processing.

To verify directly that the SICLOPPS construct produces CPs in yeast, we purified the encoded CP from yeast lysates by virtue of its His-Pro-Gln (HPQ) motif. This sequence has a well established streptavidin affinity, which was previously used to purify spliced CPs from bacterial cultures[27]. We used streptavidin agarose to pull down the HPQ CP from lysates of stationary-phase yeast and confirmed its identity by MALDI and electrospray mass spectrometry. These data provide the first demonstration that the SICLOPPS construct can be used to produce CPs in yeast.

Construction of a yeast-compatible CP library

Having established that the SICLOPPS construct expresses and splices in yeast, we sought to construct a high-diversity library compatible with yeast-based selections. We used a previously described PCR cloning strategy to generate a randomized insert with a minimum of frameshift errors (see **Supplementary Methods, Supplementary Table 1** and **Supplementary Table 2**)[28]. In contrast to previous SICLOPPS libraries with smaller CP backbones, we chose to construct an octamer library to maximize diversity and minimize effects of side chains on splicing efficiency[6,8,12]. The library was designed to encode CP octamers with a single cysteine residue followed by seven randomized residues, as a nucleophile at the first position is required for the transesterification step of intein processing[24]. After transformation into bacterial cells, the total diversity of the library (as measured by counting the number of independent transformants by serial dilution) was 5×10^7 independent members.

Library quality was assessed by picking and analyzing 20 colonies at random (**Fig. 1c** and **Supplementary Table 2**). Sequencing showed that library constructs encoded CPs with high diversity at the protein sequence level. Sequence data also confirmed that the library possessed low background: only 1 of 20 clones was the original HPQ-encoding vector, 3 of 20 possessed frameshift mutations, and 1 of 20 had a stop codon in the randomized region. Thus, we estimate ~75% (15 of 20) of the library to encode novel CPs.

We next assessed expression and processing of each of the 20 randomly picked constructs. The laboratory yeast strain W303 was individually transformed with each of the 20 constructs, grown to log phase and lysed. Western blots of these lysates revealed that all fifteen of the novel CP constructs expressed. Fourteen showed evidence of some processing at log phase, most of them quite robustly (**Fig. 1c**). This quality control analysis indicated that roughly 70% of the library encoded CP constructs that expressed and underwent intein processing in yeast. These more than 30 million potential CPs represent a diverse and largely unexplored chemical space ready for screening or selection.

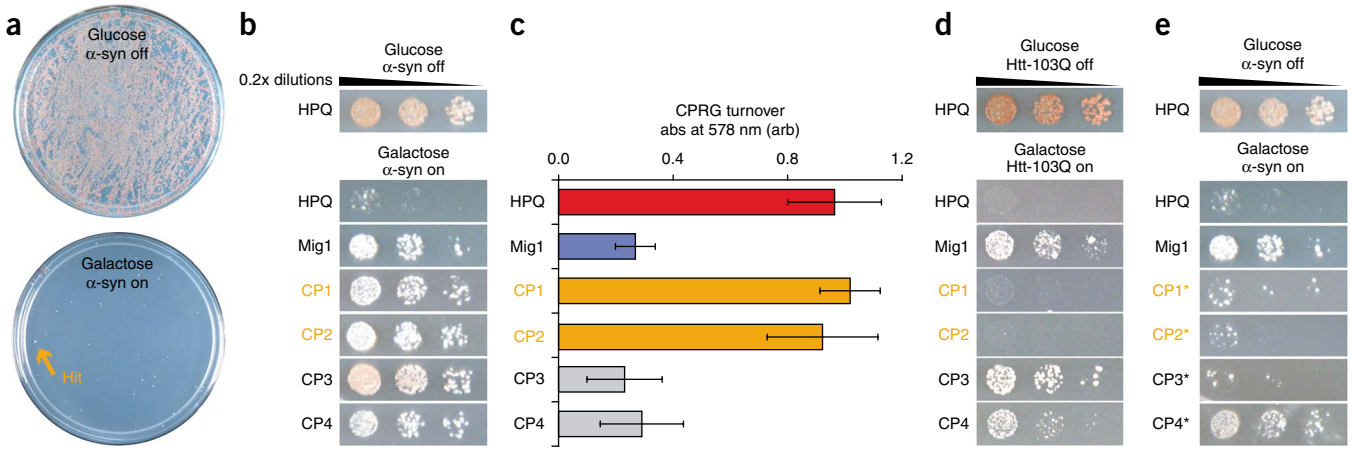

Figure 2 Identification of two CPs that selectively reduce α-synuclein toxicity in yeast. (**a**) The α-syn selection strain was transformed with the CP library, allowed to recover, and replated on galactose medium to induce α-syn expression. Glucose and galactose plates are shown to illustrate how a single robust hit clone was isolated from >150,000 transformants on a single plate. (**b**) After isolation and amplification in bacteria, hit plasmids were individually transformed into the screening strain. Transformants were allowed to recover, normalized for cell number, serially diluted and plated on galactose medium. Four hits, named CP1–CP4, are shown along with a negative control CP plasmid (HPQ) and the positive control Mig1, a genetic repressor of the *GAL1* promoter. (**c**) A *GAL1-lacZ* reporter assay using the soluble β-galactosidase substrate CPRG demonstrated that CP1 and CP2 did not affect protein expression. Error bars, s.d. from five independent trials. (**d**) Spotting assay, similar to **b**, demonstrating that CP1 and CP2 do not affect toxicity in a yeast strain expressing multiple copies of Htt-103Q from the *GAL1* promoter. (**e**) Spotting assay, similar to **b**, demonstrating that intein-disabled T69A H72A mutants of CP1-3 (asterisks) no longer suppressed α-syn toxicity. Thus, for these constructs, both specific CP sequences and intein processing were required for activity.

Selection in a yeast synucleinopathy model

With a diverse, high-quality library in hand, we next sought to perform selections in a complex biological system, one that would not be amenable to *in vitro* methods such as phage display. To this end, we applied the library to our yeast synucleinopathy model using a simple bulk selection protocol. The yeast synucleinopathy model uses the *GAL1* promoter to tightly control expression of human α-syn, so that no α-syn is produced until the yeast are grown on galactose medium[16,17]. We transformed 1 liter of yeast culture with 80 μg library DNA and plated it on large library plates lacking uracil (–ura) to select for transformed cells. This yielded 5 million independent transformants, which we scraped, replated on galactose medium to induce α-syn expression, and incubated for 3 d (**Fig. 2a**). Ninety-six large colonies were picked, and the corresponding plasmids were isolated, amplified in bacteria and individually retested in the screening strain. Thirty-one clones demonstrated reproducible suppression of α-syn toxicity in yeast (four shown in **Fig. 2b**). False positives probably stemmed from spontaneous genomic suppressor mutations, which are common in most yeast selections[17,29].

Filtering assays

We further evaluated the 31 selected CP constructs using two secondary assays to exclude promoter effects and other nonspecific modes of action. First, the constructs were transformed into a reporter yeast strain with the *lacZ* gene downstream of the *GAL1* promoter[30]. Expression of β-galactosidase from the *GAL1* promoter was then quantified using the soluble β-galactosidase substrate chlorophenol red–β-D-galactopyranoside (CPRG). This enabled us to quantify the effects of each construct on *GAL1*-mediated expression independently of the presence of α-syn (**Fig. 2c**). Second, the constructs were transformed into a yeast disease model that uses the *GAL1* promoter for the inducible expression of a toxic polypeptide unrelated to α-syn, exon 1 of human huntingtin with 103 glutamine residues (Htt-103Q)[14,15]. The transformants were then spotted onto galactose medium to assess the abilities of selected hits to suppress the toxicity of Htt-103Q in yeast (**Fig. 2d**). This assay provided a second check on whether the constructs acted by interfering with expression from the *GAL1* promoter and also tested whether the observed effects were specific to α-syn. Of course, selected CP constructs that suppressed both α-syn and Htt-103Q toxicity could be affecting a pathway common to both[31]. However, all selected constructs that prevented Htt-103Q toxicity also reduced *GAL1*-mediated expression (for example, CP3, shown in **Fig. 2b**,**c**). Two of the 31 selected constructs, denoted CP1 and CP2, suppressed α-syn toxicity but had no effects in the *GAL1* reporter assay or on Htt-103Q toxicity, and thus were acting by an α-syn-specific mechanism. Notably, these results are in keeping with our previous results from genetic screens, in which genes that suppress α-syn toxicity possess little overlap with genes that suppress Htt-103Q toxicity[15,17]. Thus, suppressors such as CP1 and CP2 affect specific pathways of eukaryotic cell biology involved in the toxicity of these human proteins, rather than nonspecific pathways involved in general protection from misfolded or aggregated proteins.

At this point we sought to ensure that the spliced CPs, rather than nucleic acid or peptide aptamers encoded by the selected constructs, were responsible for the observed suppression of α-syn toxicity. To this end, we performed three independent tests to ensure that complete splicing was required. We first tested T69A H72A mutants of each construct, which are unable to process at the extein/N-intein junction[24,25]. T69A H72A mutants of CP1 and CP2 were unable to suppress α-syn toxicity (**Fig. 2e**). Next, a different set of mutations at residues His24 and Phe26 in the *dnaE* C-intein domain (responsible for promoting asparagine cyclization in the final processing step at the extein/C-intein junction)[24,32] also abolished the activities of CP1 and CP2 (**Supplementary Results** and **Supplementary Fig. 1**). Thus, the complete splicing mechanism, including processing at both the N-intein and C-intein junctions, was required for CP1 and CP2 activity. Finally, to completely rule out the possibility that linear peptide byproducts are responsible for suppression of α-syn toxicity, we also directly tested alternative constructs that represent products of an N-intein cleavage event rather than complete cyclization. These

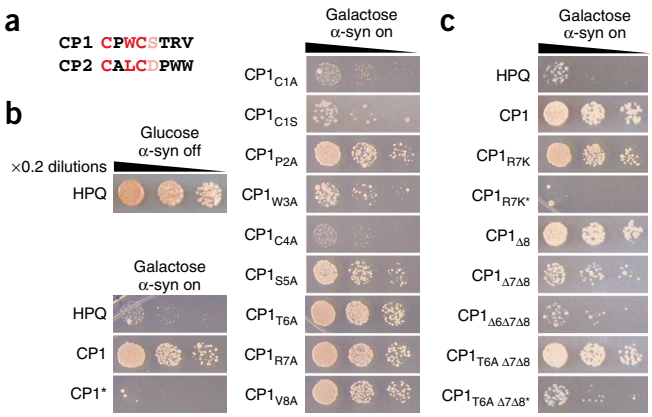

Figure 3 Rapid generation of structure–activity relationship data and rapid minimization using point mutagenesis. (**a**) Sequences of the CPs encoded by CP1 and CP2. Red, residues found by SAR analysis to be required for function; pink, residues with minor contributions. (**b**) Spotting assays of normalized, serially diluted cells of the screening strain expressing the negative control HPQ, the selected construct CP1, indicated point mutants of CP1, and the intein-disabled T69A H72A mutant CP1*. Each construct was verified to express and process in yeast. Similar results were obtained for CP2 (**Supplementary Fig. 3**). (**c**) Spotting assays of yeast expressing HPQ, CP1 and further CP1 variants. These variants illustrate incorporation of a chemical handle (lysine substitution at position 7) as well as minimization of the size of the encoded CP. Each construct was verified to express and process in yeast. Asterisks denote intein-disabled T69A H72A mutants, which were verified to express but not process.

constructs also failed to suppress α-syn toxicity, demonstrating that the sequences encoded by CP1 and CP2 were inactive without complete intein splicing (**Supplementary Results** and **Supplementary Fig. 2**). Notably, one of the strongest inhibitors of expression from the *GAL1* promoter, CP3, also required intein processing for function, suggesting that its mode of action is also mediated by a spliced CP.

Structure–activity relationships by point mutagenesis

A critical bottleneck in chemical genetics is the generation of useful structure–activity relationship (SAR) data once hits are identified from large libraries of compounds. An advantage of the CP approach is that SAR data can be generated rapidly and cost-effectively using point mutagenesis. We generated a series of alanine-scanning mutants to identify which side chains of CP1 and CP2 were responsible for function and to determine whether the two suppressors shared a common functional motif (**Fig. 3** and **Supplementary Fig. 3**). Each mutant was transformed into yeast, and expression and processing were verified by blotting log-phase cultures. Yeast cells expressing each mutant were serially diluted and plated on galactose medium to quantify the degree of α-syn toxicity suppression (**Fig. 3b**). We found that the cysteine in the fourth CP position was absolutely required for activity in both constructs. Mutation of the hydrophobic residue in the third CP position (tryptophan for CP1 and leucine for CP2) resulted in constructs with very weak activity. Mutation of the residue in the fifth CP position (serine for CP1 and glutamate for CP2) resulted in a reproducible decrease to one-fifth the growth seen with CP1 and CP2, indicating a possible role for these side chains as well.

Replacement of the cysteine in the first position with alanine resulted in another intein-disabled construct, as expected from the accepted mechanism of intein splicing. To test the requirement for the first cysteine thiol in the spliced CP, we mutated it to serine. These mutants expressed and processed as efficiently as the original CP1 and CP2 constructs as assessed by blotting, but did not suppress α-syn toxicity (**Fig. 3b** and **Supplementary Fig. 3**). Thus the cysteine in the first position is also required for the biological activities of selected CPs. Overall, CP1 and CP2 share a common CXΦC motif, wherein X is any residue and Φ is a hydrophobic residue.

CP backbone minimization using iterative design

We constructed an octamer CP library to provide diversity, but it was unclear whether selected hits would function only as octamers or might be amenable to minimization. Minimization of CPs would evaluate the extent to which selected functional motifs are dependent on macrocycle size and structure, and would also be desirable for downstream applications as chemical genetics agents. Having selected two functional CP constructs with a common tetrapeptide motif, we had the opportunity to test directly whether the remaining portions were necessary for proper orientation of the motif. Thus, building upon our side chain SAR data, we designed further mutants in order to minimize CP ring size.

CP1 proved especially amenable to minimization (**Fig. 3c**). Residue 8 could be deleted entirely with no loss of function. However, a construct with both residues 8 and 7 deleted showed only minimal function and a construct with residues 8, 7 and 6 deleted showed no ability to rescue α-syn toxicity. Because the side chains of these residues were not required for function, we hypothesized that conformational effects on the CXΦC motif were responsible for the loss of function. To restore proper orientation in the context of the hexamer, we tested a variety of substitutions in positions 2, 5 and 6, including glycine, alanine, proline, lysine and tryptophan. Of the 12 mutants tested, substitution of the threonine at position 6 with alanine or glycine had the greatest effect, restoring the ability to suppress α-syn toxicity to one comparable to that of the original eight-residue CP1 (**Fig. 3c**). We also tested intein-disabled mutants of these constructs to ensure that the activity was still dependent on intein processing.

Overall, two rounds of rationally designed mutagenesis generated constructs encoding CP hexamers that suppressed α-syn toxicity equally well as the selected CP octamers CP1 and CP2. Thus, simple iterative testing of designed mutants was used to minimize the originally selected eight-residue CP (predicted MW = 933) to a six-residue CP (predicted MW = 634) with no observable change in *in vivo* activity.

CPs are easily incorporated into affinity reagents

Target identification is another notoriously difficult hurdle in forward chemical genetics[33]. CPs are readily synthesized in several-milligram quantities and easily derivatized, making them ideal for physical pull-down experiments. Because CPs have no free N termini, lysine amines would represent useful handles for site-specific derivatization or attachment to solid phase. We verified genetically that incorporation of a lysine at position 7 did not affect CP function (**Fig. 3c**), then synthesized $CP1_{R7K}$ (**1**) and $CP2_{W7K}$ (**2**) (**Supplementary Fig. 4** and **Supplementary Methods**). We linked the synthetic CPs to agarose beads and optimized pulldown conditions (**Supplementary Methods**). Notably, because the CPs were hydrophilic, high lysate protein concentrations (5–10 mg ml^{-1}) could be used without extensive nonspecific binding.

Proteins that selectively bound CP1- or CP2-linked beads over control CP–linked beads were eluted, separated by SDS-PAGE, and identified by mass spectrometry. Yeast genetics streamlines the process of validating potential targets, and so we were able to rapidly test several target candidates. However, modulation of the amounts of these proteins in yeast by genetic overexpression or deletion did not affect

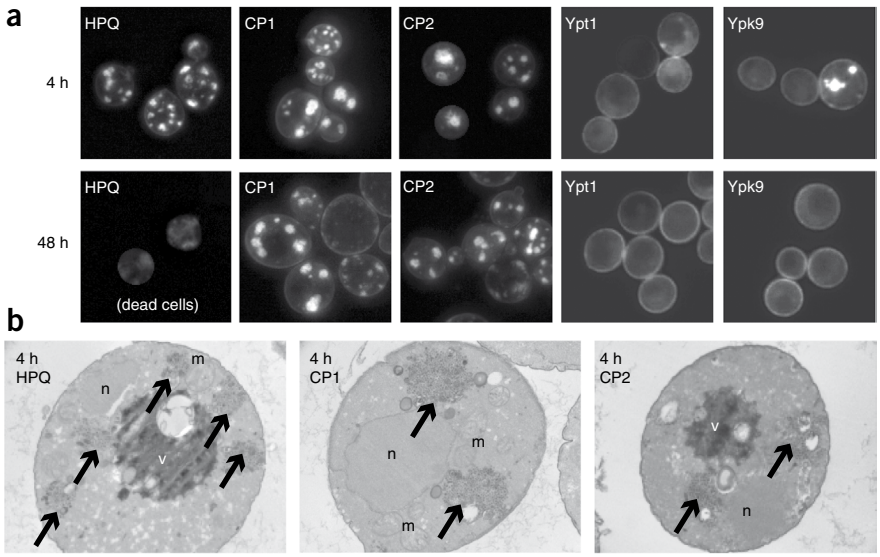

Figure 4 Selected CPs operate downstream of known vesicle trafficking defects. (**a**) Representative fluorescence micrographs of cells expressing α-syn–YFP after 4 h (top row) or 48 h (bottom row), along with the indicated CP or yeast gene. (**b**) Representative electron micrographs of cells expressing α-syn–YFP after 4 h, along with the indicated CP. m, mitochondrion; *n*, nucleus; v, vacuole; arrows, pools of stalled vesicles. White ovals are lipid droplets.

α-syn toxicity or CP-mediated suppression of α-syn toxicity. We also readily linked $CP1_{R7K}$ and $CP2_{W7K}$ to biotin and to photoactivatable cross-linking groups but were unable to selectively isolate more target candidates. There are three likely explanations for these results. First, CP targets may be transient, unstable or present in small amounts within the cell. Second, selected CPs may possess low affinities for their targets, as CPs selected in bacteria have shown high micromolar K_i and IC_{50} (half-maximal inhibitory concentration) values in *in vitro* assays[6,34]. Finally, CP1 and CP2 may act by a nontraditional mechanism that is incompatible with physical target identification. Our results demonstrate that the preparation of CP-based affinity reagents can be rapid and straightforward. We are now exploring further methods to translate this capability into similarly rapid techniques for target identification.

CP1 and CP2 are unique suppressors of α-syn toxicity

Previous work using the yeast model has established that overexpression of human α-syn affects specific steps in vesicle trafficking[18]. We wondered whether our selected CPs act upstream or downstream of these defects. The yeast synucleinopathy model is particularly useful for examining the effects of α-syn on vesicle trafficking because α-syn induction can be tightly controlled and α-syn localization within the cell can be monitored in real time using yellow fluorescent protein (YFP) fusions[17,18]. Shortly after induction, α-syn–YFP accumulates on the plasma membrane. After 2–3 h of α-syn–YFP induction, small foci are observed peripherally to the membrane, and after 4–6 h these foci coalesce and begin to migrate inward toward the vacuole. This latter stage is associated with the onset of cell death. Immunoelectron microscopy has revealed that these foci correspond to pools of stalled vesicles that are coated with α-syn–YFP[18].

We wondered whether CP1 and CP2 prevent the accumulation of pools of stalled vesicles, as previously described genetic suppressors of α-syn toxicity mitigate the trafficking blockage[17]. For instance, the expression of a Rab homolog involved in endoplasmic reticulum–Golgi trafficking (Ypt1) or the yeast homolog of the P-type ATPase encoded by *PARK9* (Ypk9) suppresses α-syn–YFP foci[17,18,22]. By contrast, CP1 and CP2 did not alter the occurrence or appearance of α-syn–YFP foci after 4 h (**Fig. 4a**). Electron microscopy confirmed that cells expressing CP1 or CP2 along with α-syn still had pools of stalled vesicles similar to those found in cells expressing a negative control CP along with α-syn (**Fig. 4b**). Notably, even though 8–12 h of α-syn–YFP induction was lethal to control cells, CP1 and CP2 possessed α-syn–YFP foci continuously for over 48 h after induction, with little change in appearance after 8 h (**Fig. 4a**). Thus, CP1 and CP2 permitted cells to grow and divide, albeit at a reduced rate, despite the continuous presence of stalled α-syn-coated vesicles. This phenotype is, to our knowledge, unique among the genetic and small molecule suppressors of α-syn toxicity identified so far, and implies that the selected CPs target a pathway downstream of established vesicle trafficking defects[17,18,22,31].

The previously described genetic suppressors Ypt1 and Ypk9 act in independent pathways from each other, so that the simultaneous expression of both genes results in more potent suppression of α-syn toxicity than the expression of either gene by itself[22]. To genetically test whether selected CPs act in yet another pathway, we expressed them in combination with Ypt1 or Ypk9. The effects of CP1 and CP2 combined additively with the effects of either of these genetic suppressors (**Supplementary Results** and **Supplementary Fig. 5**). Thus, the CPs are likely to act in pathways that are distinct from those already linked to α-syn toxicity.

Expression of CPs in a metazoan animal model

We have previously demonstrated that human homologs of suppressors of yeast α-syn toxicity identified are able to rescue dopaminergic neurons in animal models of synucleinopathy, including a *C. elegans* whole-animal model and a *Rattus norvegicus* primary midbrain model[17,18,22]. In the *C. elegans* model, expression of human α-syn from the dopamine transporter promoter $P_{dat\text{-}1}$ results in degeneration of dopaminergic neurons[18,35,36]. This enables direct evaluation of putative α-syn antagonists in dopaminergic neurons in the context of whole animals. Nematode development is highly stereotyped and reproducible, so that any alteration in neuron quantity or morphology is highly significant. Nematodes are also transparent, enabling assessment and scoring of dopaminergic neurons in live worms by virtue of GFP expression under the control of the $P_{dat\text{-}1}$ promoter. Using this model, we have found that expression of genes such as *Rab1* and *PARK9* (homologs of *ypt1* and *ypk9*) ameliorate α-syn toxicity in the dopaminergic neurons of live worms[18,22,36].

We sought to evaluate whether CP1 and CP2 would similarly rescue dopaminergic neurons in the nematode synucleinopathy model. Because the original split intein was isolated from a cyanobacterium, we first codon-optimized and resynthesized the entire gene to ensure efficient expression in metazoan systems such as *C. elegans* and mammalian cells. Then $P_{dat\text{-}1}$*::mCP-gfp* expression vectors were constructed by recombinational cloning with the pDEST-DAT-1 destination vector[35] to generate a construct that would express the metazoan-optimized CP (mCP) gene with a C-terminal GFP fusion in nematode dopaminergic neurons.

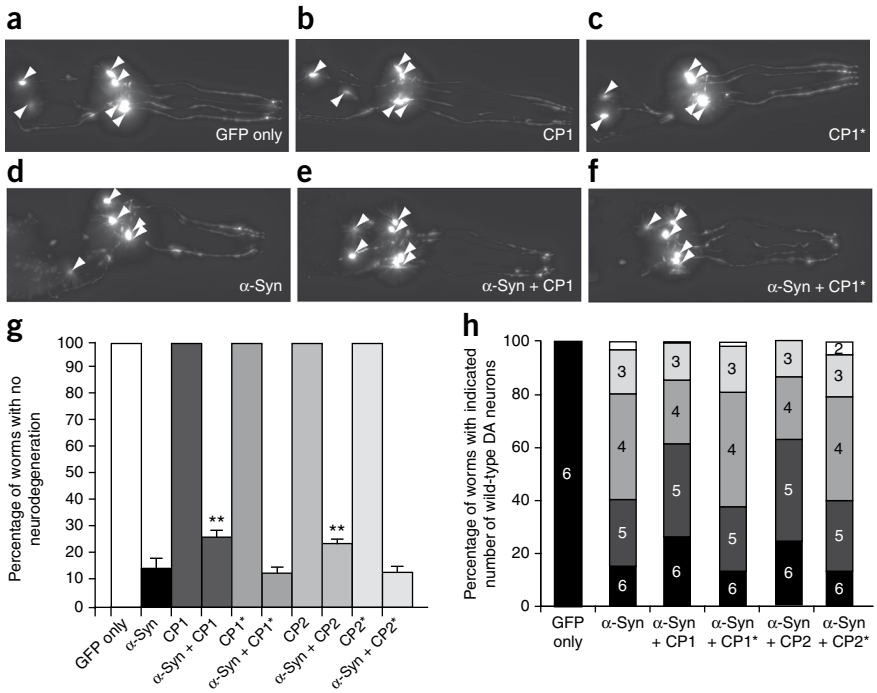

Figure 5 Selected CPs reduce α-syn-mediated toxicity in *C. elegans* dopaminergic neurons. (**a**–**f**) Representative fluorescence micrographs of isogenic worm strains with GFP expression in dopaminergic neurons. Arrowheads, cell bodies; processes are visible to the right. (**a**) At 7 d old, worms showed six intact anterior dopaminergic neurons. (**b**,**c**) Expression of CP1 and the intein-disabled CP1* constructs in anterior dopaminergic neurons had no discernable effect on neuron health or development in the absence of α-syn. (**d**) Most worms expressing α-syn had missing or degenerated anterior dopaminergic neurons. (**e**) CP1 protected the dopaminergic neurons from α-syn-induced neurodegeneration, resulting in a greater proportion of worms, like the representative one shown, with no degeneration in all four CEP and two ADE neurons. (**f**) Expression of the intein-disabled CP1* construct does not afford the same protection as CP1. (**g**) Population analysis; 26% and 24% of worms expressing CP1 and CP2, respectively, showed no neurodegeneration, compared with only ~15% of control worms expressing only α-syn or expressing intein-disabled constructs CP1* and CP2* (** $P <$ 0.05, Student's *t*-test). Error bars, s.d. of three trials with three independently generated worm lines, $n = 90$ for each line, making a total of 270 worms examined for each transgenic strain. (**h**) Distributions of worms by number of intact, wild-type dopaminergic neurons revealed that selected CPs also reduced the severity of the observed neurodegeneration, preferentially rescuing the two more sensitive ADE neurons.

First, to verify that the mCP construct is expressed in the dopaminergic neurons of *C. elegans*, we injected $P_{dat\text{-}1}$::*mCP-gfp* expression vectors into wild-type worms. Because nematodes have only eight dopaminergic neurons, detection of gene products expressed exclusively in these few cells by western blotting is problematic. However, GFP fusions allow direct observation of protein expression in live worms. Expression of mCP-GFP started during embryogenesis, and in adult worms robust GFP fluorescence was observed selectively in dopaminergic neurons (**Supplementary Fig. 6**). Because the GFP is encoded downstream of the mCP gene, we inferred that the mCP gene expresses in *C. elegans* dopaminergic neurons.

CP1 and CP2 suppress α-syn toxicity in dopaminergic neurons

We next tested the effects of expressed CP1 and CP2 on α-syn-mediated dopaminergic neuron loss in *C. elegans*. The CP1 and CP2 sequences were introduced into mCP genes without GFP fusions by site-directed mutagenesis and the resulting constructs were cloned into the pDEST-DAT-1 vector[35]. We generated transgenic worm lines using these expression vectors as described[17,36]. We also constructed and tested negative controls, denoted CP1* and CP2*, with the intein-disabling T69A H72A mutation.

We quantified the effects of mCP constructs on α-syn toxicity as previously described for human and nematode genes, staging individual worms and inspecting the six anterior dopaminergic neurons (**Fig. 5**)[17,18,36]. Expression of all mCP constructs had no discernable effect on neuron health or morphology in the absence of α-syn, indicating that the mCP gene is well tolerated by live worms in dopaminergic neurons (**Fig. 5a–c**,**g**). As previously described, GFP expression also had no effect on dopaminergic neurons, whereas α-syn expression caused substantial dopaminergic neurodegeneration (**Fig. 5d**,**g**)[17,18,22,36]. Only 15% of 7-d-old worms expressing α-syn retained wild-type numbers and morphologies of dopaminergic neurons. Expression of mCP constructs encoding either CP1 or CP2 in these worms significantly reduced dopaminergic neurodegeneration, raising the proportions of worms devoid of neurodegeneration to 26% and 24%, respectively (**Fig. 5e**,**g**). Intein-disabled variants CP1* and CP2* were ineffective (**Fig. 5f**,**g**).

We also quantified the severity of the neurodegeneration by counting the number of healthy dopaminergic neurons in each worm studied. We observed that 15% of worms expressing α-syn alone retained all six anterior dopaminergic neurons, while 40% retained five or more and 80% retained four or more (**Fig. 5h**). CP1 and CP2 significantly increased the proportion of worms with all six dopaminergic neurons intact and the proportion of worms that retained five or more dopaminergic neurons, consistent with our observations that worms expressing α-syn are most susceptible to degeneration in their two ADE neurons, and less susceptible in their four anterior CEP neurons[18,22,36]. Quantifying the numbers of healthy dopaminergic neurons in worms expressing intein-disabled variants CP1* and CP2* showed distributions similar to those in worms expressing α-syn alone, again demonstrating that intein processing was required for the observed activities of the CP1 and CP2 constructs.

DISCUSSION

We report a rapid and versatile technique for the *in vivo* selection of bioactive CPs in yeast. Our CP octamer library encodes diverse macrocycles of molecular weights from ~600 to 1,200 Da and can be effectively introduced into any yeast strain, including models of human disease. Hits can be rapidly identified using selections or screens that sort millions of CPs in a single day without expensive robotics. In selections using our yeast synucleinopathy model, we isolated two hits from an original pool of 5 million after only a single round of selection. Although more rounds of selection were not required for selections in the synucleinopathy model, we note that multiple rounds of selection could be performed by pooling colonies and amplifying their plasmids *en masse*. Stringency of the selection

could be increased in subsequent rounds by using more robust selection conditions or by transferring selected CP genes to expression vectors with weaker promoters.

We also report the first expression of optimized mCP genetic constructs in live metazoans and their effectiveness in suppressing α-syn toxicity in *C. elegans* dopaminergic neurons. Notably, the extents to which CP1 and CP2 reduced the amount and severity of dopaminergic neurodegeneration matched those of human homologs of hits from our yeast genetic screen[17]. These include Rab GTPases critical for proper vesicle trafficking and *PARK9*, a human gene linked to a genetic, early-onset form of parkinsonism[17,18,22,23]. Thus, in yeast and *C. elegans* synucleinopathy models, selected CPs were as potent as endogenous regulators of key cellular pathways implicated in Parkinson's disease.

The ability to use mutagenesis to generate SAR data and the straightforward synthesis of CPs greatly streamlines the turnaround of hits into affinity reagents for target identification. The time from initial selections to affinity reagent in hand was less than two months. Physical pull-downs have not yet revealed a clear target or targets for CP1 and CP2, but various alternatives are being used to identify their modes of action. For instance, we are now developing CPs with higher potency by designing more stringent selections and applying second-generation libraries that incorporate the CXΦC motif. We are also exploring whether CP1 and CP2 reduce α-syn toxicity by buffering the thiol redox state of the cytosol or by otherwise altering the activity of thioredoxin-fold proteins[37]. These possibilities are suggested by the noteworthy similarity between the CXΦC motif and the thioredoxin-fold CXXC motif, the critical roles of thiol redox pathways in endoplasmic reticulum stress (which is a prominent effect of α-syn expression), and previous findings that dithiol small molecules, peptides and small CPs have biologically relevant thiol redox potentials that vary greatly depending on neighboring functional groups and backbone conformation[37–40]. The CXΦC motif may also function by binding metal ions, as metal ion transporters were discovered among the genetic suppressors and enhancers of α-syn toxicity and manganese exposure has long been known as a risk factor for Parkinson's disease–like syndromes[22,41]. Either of these possibilities would represent new proteostasis-based mechanisms that would defy physical target identification. Finally, a variety of genetic and genomic tools are available for target identification in yeast, including transcriptional profiling, genetic screening and the use of libraries of bar-coded overexpression and deletion strains[33,42]. All of these strategies will be applied to CP1 and CP2.

CPs selected in the yeast synucleinopathy model produced a phenotype unexpected and, to our knowledge, unique, apparently acting downstream of α-syn-mediated vesicle trafficking defects. Moreover, CP1 and CP2 acted independently of known genetic suppressors of α-syn toxicity, and were effective in both yeast and nematode synucleinopathy models. This provides critical evidence that the target pathways are indeed conserved and relevant to the pathobiology of α-syn in neurons. Whether they act by binding a specific protein or by modulating thiol or metal homeostasis, CP1 and CP2 represent a promising new avenue of exploration for therapeutics for Parkinson's disease and other synucleinopathies. Moving forward, the successful application of the new mCP construct in an animal opens the door to further validation in other Parkinson's disease models, including viral introduction into cell culture and incorporation in transgenic mice[18,22,43].

Overall, the CP approach represents a technology for the rapid development of chemical genetics agents for systems that are difficult to address *in vitro*. In addition, the abundance of established yeast two-hybrid selection strains, already validated in explorations of the binary interactomes of yeast, *C. elegans* and human, will enable rapid and low-cost selections for CP inhibitors of specific protein–protein interactions on a large scale[44–46]. Our approach provides a powerful alternative to traditional small molecule screening, straying from traditional 'drug-like' chemical space but offering higher throughput and lower cost. It also possesses distinct advantages over display technologies, requiring fewer rounds of selection, obviating the need to purify and immobilize the target, and enabling selections *in vivo*, albeit with lower throughput. These trade-offs will appeal to biologists interested primarily in developing tools for probing specific cellular pathways and identifying key druggable proteins in disease models.

METHODS

Yeast strains, manipulation, selections and blotting. The α-syn-expressing yeast strains used in this study were all haploid W303 strains with the following genotype: *MATa can1-100 his3-11,15 leu2-3,112 trp1-1 ura3-1 ade2-1*. Selections and SAR data generation were performed in the previously described IntTox strain, which has human α-syn integrated using pRS303-αSynWT-YFP and pRS304-αSynWT-YFP vectors[17]. Expression of CPs together with genetic suppressors was performed using the related HiTox strain, in which human α-syn is integrated using pRS304-αSynWT-GFP and pRS306-αSynWT-GFP vectors[16]. The Htt-103Q strain used was similarly constructed from the W303 background using integrated pRS303-Htt103Q-GFP and pRS305-Htt103Q-GFP constructs as described[14].

Yeast cultures were transformed using standard lithium acetate heat shock. In all cases, at least three independent transformants were isolated and tested to ensure reproducibility of the resulting phenotype. Library transformations were performed using a scaled-up heat shock procedure. One liter of IntTox yeast were grown to log phase in SC –His –Trp medium (6.7 g l^{-1} Yeast Nitrogen Base (BD Biosciences), appropriate amino acid dropout mix (Sunrise Science Products), 2% (w/v) glucose), pelleted and washed several times with water. Pellets were resuspended in 20 ml of 0.1 M lithium acetate and incubated for 20 min at 30 °C with shaking. Cells were then spun down and resuspended in 10 ml of 0.1 M lithium acetate with 10 mM Tris-Cl, pH 7.5, and 1 mM EDTA. Eighty micrograms library DNA were added along with 1.4 ml of carrier DNA (salmon sperm DNA, 2 mg ml^{-1}, previously boiled and kept on ice) and 25 ml of 50% (w/v) polyethylene glycol (relative molecular mass 4,000). After 30 min of incubation at 30 °C with shaking, 3 ml of DMSO were added and the cells were heat shocked at 42 °C for 23 min. Cells were pelleted and resuspended in water before plating on 24.5 × 24.5 cm Petri dishes of SC –His –Trp –ura solid medium. After 2 d, all colonies were scraped and pooled, and 150,000–200,000 cells were plated on each of 35 SGal –His –Trp –ura plates (identical to SC plates but with 2% (w/v) galactose rather than glucose). Picked colonies were cultured overnight in SC –ura and pelleted. Plasmids were isolated using the PrepEase yeast plasmid isolation kit (USB).

Cultures for blotting were produced by growing cultures until saturation, diluting to an absorbance at 600 nm (A_{600}) of 0.1 and growing for 4–5 h. Lysates were produced by bead-beating pelleted cells in ethanol with 1 mM PMSF, removing the ethanol by evaporation in a Speed-Vac (Savant) and resuspending in 20 mM Tris, pH 6.8, with 2% (w/v) SDS. These were then normalized by protein concentration using a BCA assay (Pierce), mixed with SDS-free loading buffer and subjected to SDS-PAGE and blotting onto PVDF membranes. Blots were probed with antiserum to the chitin-binding domain (New England Biolabs) or with purified antibody to the hemagglutinin tag (Sigma) according to standard protocols.

HPQ cyclic peptide isolation. Log-phase cultures expressing the HPQ-encoding SICLOPPS construct were spun down and resuspended in 50 mM Tris, pH 7.5, 150 mM NaCl, 1 mM EDTA, with protease inhibitors (Roche) and 1 mM DTT. Cells were lysed by passing through a French press at 10,000 p.s.i. twice. Lysates were incubated with streptavidin-agarose beads for 4 h at 4 °C and washed extensively. Biotin (1 mM) was used to elute the HPQ cyclic peptide. Eluates were freeze-dried using a Speed-Vac (Savant) and resuspended in 10 μl 50:50 water/acetonitrile with 0.1% (v/v) formic acid. These were

further cleaned using C18 ZipTips (Millipore) and analyzed by MALDI-MS (expected molecular mass plus proton = 1,330.6, observed molecular mass plus proton = 1,330.5, a discrepancy well within experimental tolerance) as well as electrospray mass spectrometry (expected molecular mass plus proton = 1,330.6, observed molecular mass plus proton = 1,330.6).

Colorimetric *lacZ* assay in yeast. Cells with a freshly integrated *GAL1*::*lacZ* construct were used to assess the effects of isolated CP constructs on expression from the *GAL1* promoter[30]. Samples were prepared by growing cells overnight in raffinose medium, then diluting to an A_{600} of 0.1 and growing for 4–8 h in galactose medium to induce *lacZ* expression. Alternatively, cells were plated onto galactose plates and individual colonies picked after 36–48 h. Both methods produced similar results; data shown (**Fig. 2c**) are from picked colonies because of the ease with which many independent clones could be analyzed. Cells were spun down, washed with water and normalized to an A_{600} of 0.4–0.8 in 110 µl in wells of a 96-well plate. 90 µl of CPRG solution (100 mM HEPES, pH 7.25, 150 mM NaCl, 0.65 mg ml^{-1} L-aspartate, 0.01 mg ml^{-1} bovine serum albumin (Sigma), 0.05% (v/v) Tween-20 (Sigma), 0.5% (w/v) SDS, 0.75 mg ml^{-1} chlorophenol red–β-D-galactopyranoside (Sigma)) was added to each well. Plates were shaken at room temperature for 30–120 min. Plates were read at 578 nm and normalized for absorbance due to yeast optical density.

***C. elegans* strain generation and analysis of dopaminergic neuron degeneration.** Nematodes were maintained following standard procedures[47]. The transgenic strains UA109 (baInl1[$P_{dat\text{-}1}$::a-syn; $P_{dat\text{-}1}$::gfp]; baEx84 [$P_{dat\text{-}1}$::mCP_CP1; *rol-6* (su1006)]), UA110 (baInl1[$P_{dat\text{-}1}$::a-syn; $P_{dat\text{-}1}$::gfp]; baEx85[$P_{dat\text{-}1}$::mCP_CP1*; *rol-6* (su1006)]), UA111 (baInl1 [$P_{dat\text{-}1}$::a-syn; $P_{dat\text{-}1}$::gfp]; baEx86[$P_{dat\text{-}1}$::mCP_CP2; *rol-6* (su1006)]), UA112 (baInl1[$P_{dat\text{-}1}$::a-syn; $P_{dat\text{-}1}$::gfp]; baEx87[$P_{dat\text{-}1}$::mCP_CP2*; *rol-6* (su1006)]), UA119 (vtIs1[$P_{dat\text{-}1}$::gfp; *rol-6* (su1006)]; baEx93[$P_{dat\text{-}1}$::mCP_CP1; $P_{unc\text{-}54}$::mCherry]), UA120 (vtIs1[$P_{dat\text{-}1}$::gfp; *rol-6* (su1006)]; baEx94[$P_{dat\text{-}1}$:: mCP_CP1*; $P_{unc\text{-}54}$::mCherry]), UA121 (vtIs1[$P_{dat\text{-}1}$::gfp; *rol-6* (su1006)]; baEx95[$P_{dat\text{-}1}$::mCP_CP2; $P_{unc\text{-}54}$::mCherry]) and UA122 (vtIs1[$P_{dat\text{-}1}$::gfp; *rol-6* (su1006)]; baEx96[$P_{dat\text{-}1}$::mCP_CP2*; $P_{unc\text{-}54}$::mCherry]) were generated by directly microinjecting 50 µg ml^{-1} expression plasmids encoding cyclic peptide and 50 µg ml^{-1} *rol-6* or $P_{unc\text{-}54}$::mCherry marker into either the integrated UA44 (baInl1[$P_{dat\text{-}1}$::a-syn; $P_{dat\text{-}1}$::gfp]) strain or the integrated BY200 (vtIs1[$P_{dat\text{-}1}$::gfp; *rol-6* (su1006)]) as a control for toxicity[48]. Three independent transgenic lines of worms were generated for each strain. Age-synchronized worms were obtained and analyzed at the indicated time as described previously[18,36]. We examined the six anterior dopaminergic neurons (four CEP and two ADE neurons) of 30 worms per trial for neurodegeneration when the worms were 7 d old. After three trials, 90 worms for each line had been analyzed, making a total of 270 worms analyzed for each transgenic strain. If a worm showed at least one degenerative change (dendrite or axon loss, cell body loss), we scored the worm as showing degenerating neurons[35,36]. For each trial, 30 worms were transferred onto a 2% agarose pad, immobilized with 2 mM levamisole, and analyzed using a Nikon Eclipse E800 epifluorescence microscope equipped with Endow GFP HYQ filter cube (Chroma). Images were captured with a Cool Snap CCD camera (Photometrics) driven by MetaMorph software (Universal Imaging).

Note: Supplementary information and chemical compound information is available on the Nature Chemical Biology website.

ACKNOWLEDGMENTS

We thank S. Benkovic (Pennsylvania State University) for plasmids, E. Spooner for mass spectrometry assistance and N. Azubuine for preparation of media. This work was supported by a National Research Service Award fellowship from the US National Institute of Neurological Disorders and Stroke (NINDS) and National Institute on Aging (J.A.K.), an R21 grant from NINDS (S.L. and J.A.K.) and the Morris K. Udall Centers of Excellence for Parkinson's Disease Research (S.L.) Parkinson's disease research in the Caldwell Lab (G.A.C, K.A.C., S.H.) was supported by the American Parkinson Disease Association, Michael J. Fox Foundation and US National Institute of Environmental Health Sciences.

AUTHOR CONTRIBUTIONS

J.A.K. conceived the overall strategy, tested the construct in yeast, designed and constructed the library, performed the selections and all subsequent experiments in yeast, constructed the metazoan CP construct and worm expression plasmids and wrote the manuscript. S.H. constructed the worm lines, designed and performed the worm experiments, analyzed worm data and wrote the manuscript. J.M.M. processed and imaged yeast by electron microscopy. S.S. contributed to the design of the metazoan CP construct. T.A.N. designed and tested the HPQ yeast CP construct. K.A.C. analyzed worm data and wrote the manuscript. G.A.C. designed the worm experiments, analyzed worm data and wrote the manuscript. S.L. suggested the approach, provided advice and suggestions throughout and supervised the project.

Published online at http://www.nature.com/naturechemicalbiology/.
Reprints and permissions information is available online at http://npg.nature.com/reprintsandpermissions/.

1. Driggers, E.M., Hale, S.P., Lee, J. & Terrett, N.K. The exploration of macrocycles for drug discovery — an underexploited structural class. *Nat. Rev. Drug Discov.* **7**, 608–624 (2008).
2. Burja, A.M., Banaigs, B., Abou-Mansour, E., Burgess, J.G. & Wright, P.C. Marine cyanobacteria—a prolific source of natural products. *Tetrahedron* **57**, 9347–9377 (2001).
3. Wilson, D.S., Keefe, A.D. & Szostak, J.W. The use of mRNA display to select high-affinity protein-binding peptides. *Proc. Natl. Acad. Sci. USA* **98**, 3750–3755 (2001).
4. Kehoe, J.W. & Kay, B.K. Filamentous phage display in the new millennium. *Chem. Rev.* **105**, 4056–4072 (2005).
5. Scott, C.P., Abel-Santos, E., Wall, M., Wahnon, D.C. & Benkovic, S.J. Production of cyclic peptides and proteins in vivo. *Proc. Natl. Acad. Sci. USA* **96**, 13638–13643 (1999).
6. Horswill, A.R., Savinov, S.N. & Benkovic, S.J. A systematic method for identifying small-molecule modulators of protein-protein interactions. *Proc. Natl. Acad. Sci. USA* **101**, 15591–15596 (2004).
7. Horswill, A.R. & Benkovic, S.J. Cyclic peptides, a chemical genetics tool for biologists. *Cell Cycle* **4**, 552–555 (2005).
8. Scott, C.P., Abel-Santos, E., Jones, A.D. & Benkovic, S.J. Structural requirements for the biosynthesis of backbone cyclic peptide libraries. *Chem. Biol.* **8**, 801–815 (2001).
9. Tavassoli, A. *et al.* Inhibition of HIV budding by a genetically selected cyclic peptide targeting the Gag-TSG101 interaction. *ACS Chem. Biol.* **3**, 757–764 (2008).
10. Cheng, L. *et al.* Discovery of antibacterial cyclic peptides that inhibit the ClpXP protease. *Protein Sci.* **16**, 1535–1542 (2007).
11. Nilsson, L.O., Louassini, M. & Abel-Santos, E. Using siclopps for the discovery of novel antimicrobial peptides and their targets. *Protein Pept. Lett.* **12**, 795–799 (2005).
12. Kinsella, T.M. *et al.* Retrovirally delivered random cyclic peptide libraries yield inhibitors of interleukin-4 signaling in human B cells. *J. Biol. Chem.* **277**, 37512–37518 (2002).
13. Winderickx, J. *et al.* Protein folding diseases and neurodegeneration: lessons learned from yeast. *Biochim. Biophys. Acta* **1783**, 1381–1395 (2008).
14. Duennwald, M.L., Jagadish, S., Muchowski, P.J. & Lindquist, S. Flanking sequences profoundly alter polyglutamine toxicity in yeast. *Proc. Natl. Acad. Sci. USA* **103**, 11045–11050 (2006).
15. Willingham, S., Outeiro, T.F., DeVit, M.J., Lindquist, S.L. & Muchowski, P.J. Yeast genes that enhance the toxicity of a mutant huntingtin fragment or α-synuclein. *Science* **302**, 1769–1772 (2003).
16. Outeiro, T.F. & Lindquist, S. Yeast cells provide insight into alpha-synuclein biology and pathobiology. *Science* **302**, 1772–1775 (2003).
17. Cooper, A.A. *et al.* α-Synuclein blocks ER-Golgi traffic and Rab1 rescues neuron loss in Parkinson's models. *Science* **313**, 324–328 (2006).
18. Gitler, A.D. *et al.* The Parkinson's disease protein alpha-synuclein disrupts cellular Rab homeostasis. *Proc. Natl. Acad. Sci. USA* **105**, 145–150 (2008).
19. Polymeropoulos, M.H. *et al.* Mutation in the alpha-synuclein gene identified in families with Parkinson's disease. *Science* **276**, 2045–2047 (1997).
20. Spillantini, M.G. *et al.* α-Synuclein in Lewy bodies. *Nature* **388**, 839–840 (1997).
21. Lee, V.M.Y. & Trojanowski, J.Q. Mechanisms of Parkinson's disease linked to pathological alpha-synuclein: new targets for drug discovery. *Neuron* **52**, 33–38 (2006).
22. Gitler, A.D. *et al.* α-Synuclein is part of a diverse and highly conserved interaction network that includes PARK9 and manganese toxicity. *Nat. Genet.* **41**, 308–315 (2009).
23. Ramirez, A. *et al.* Hereditary parkinsonism with dementia is caused by mutations in *ATP13A2*, encoding a lysosomal type 5 P-type ATPase. *Nat. Genet.* **38**, 1184–1191 (2006).
24. Evans, T.C. Jr. & Xu, M.-Q. Mechanistic and kinetic considerations of protein splicing. *Chem. Rev.* **102**, 4869–4883 (2002).
25. Ghosh, I., Sun, L. & Xu, M.-Q. Zincinhibition of protein *trans*-splicing and identification of regions essential for splicing and association of a split intein. *J. Biol. Chem.* **276**, 24051–24058 (2001).
26. Sun, P. *et al.* Crystal structures of an intein from the split *dnaE* gene of *Synechocystis* sp. PCC6803 reveal the catalytic model without the penultimate histidine and the mechanism of zinc ion inhibition of protein splicing. *J. Mol. Biol.* **353**, 1093–1105 (2005).

27. Naumann, T.A., Savinov, S.N. & Benkovic, S.J. Engineering an affinity tag for genetically encoded cyclic peptides. *Biotechnol. Bioeng.* **92**, 820–830 (2005).
28. Tavassoli, A. & Benkovic, S.J. Split-intein mediated circular ligation used in the synthesis of cyclic peptide libraries in *E. coli*. *Nat. Protoc.* **2**, 1126–1133 (2007).
29. Bickle, M.B.T., Dusserre, E., Moncorge, O., Bottin, H. & Colas, P. Selection and characterization of large collections of peptide aptamers through optimized yeast two-hybrid procedures. *Nat. Protoc.* **1**, 1066–1091 (2006).
30. Yocum, R.R., Hanley, S., West, R. & Ptashne, M. Use of *lacZ* fusions to delimit regulatory elements of the inducible divergent *GAL1-GAL10* promoter in *Saccharomyces cerevisiae*. *Mol. Cell. Biol.* **4**, 1985–1998 (1984).
31. Outeiro, T.F. *et al.* Sirtuin 2 inhibitors rescue alpha-synuclein-mediated toxicity in models of Parkinson's disease. *Science* **317**, 516–519 (2007).
32. Ding, Y. *et al.* Crystal structure of a mini-intein reveals a conserved catalytic module involved in side chain cyclization of asparagine during protein splicing. *J. Biol. Chem.* **278**, 39133–39142 (2003).
33. Burdine, L. & Kodadek, T. Target identification in chemical genetics: the (often) missing link. *Chem. Biol.* **11**, 593–597 (2004).
34. Tavassoli, A. & Benkovic, S.J. Genetically selected cyclic-peptide inhibitors of AICAR transformylase homodimerization. *Angew. Chem. Int. Ed. Engl.* **44**, 2760–2763 (2005).
35. Cao, S., Gelwix, C.C., Caldwell, K.A. & Caldwell, G.A. Torsin-mediated protection from cellular stress in the dopaminergic neurons of *Caenorhabditis elegans*. *J. Neurosci.* **25**, 3801–3812 (2005).
36. Hamamichi, S. *et al.* Hypothesis-based RNAi screening identifies neuroprotective genes in a Parkinson's disease model. *Proc. Natl. Acad. Sci. USA* **105**, 728–733 (2008).
37. Ellgaard, L. & Ruddock, L.W. The human protein disulphide isomerase family: substrate interactions and functional properties. *EMBO Rep.* **6**, 28–32 (2005).
38. Abou-Sleiman, P.M., Muqit, M.M.K. & Wood, N.W. Expanding insights of mitochondrial dysfunction in Parkinson's disease. *Nat. Rev. Neurosci.* **7**, 207–219 (2006).
39. Cabrele, C., Fiori, S., Pegoraro, S. & Moroder, L. Redox-active cyclic bis(cysteinyl)peptides as catalysts for in vitro oxidative protein folding. *Chem. Biol.* **9**, 731–740 (2002).
40. Kersteen, E.A. & Raines, R.T. Catalysis of protein folding by protein disulfide isomerase and small-molecule mimics. *Antioxid. Redox Signal.* **5**, 413–424 (2003).
41. Olanow, C.W. Manganese-induced parkinsonism and Parkinson's disease. in *Redox-Active Metals in Neurological Disorders* vol. 1012 (ed. LeVine, S.M.) 209–223 (New York Academy of Sciences, New York, 2004).
42. Hoon, S. *et al.* An integrated platform of genomic assays reveals small-molecule bioactivities. *Nat. Chem. Biol.* **4**, 498–506 (2008).
43. van der Putten, H. *et al.* Neuropathology in mice expressing human alpha-synuclein. *J. Neurosci.* **20**, 6021–6029 (2000).
44. Rual, J.F. *et al.* Towards a proteome-scale map of the human protein-protein interaction network. *Nature* **437**, 1173–1178 (2005).
45. Yu, H. *et al.* High-quality binary protein interaction map of the yeast interactome network. *Science* **322**, 104–110 (2008).
46. Li, S. *et al.* A map of the interactome network of the metazoan *C. elegans*. *Science* **303**, 540–543 (2004).
47. Brenner, S. Genetics of *Caenorhabditis elegans*. *Genetics* **77**, 71–94 (1974).
48. Nass, R., Hall, D.H., Miller, D.M. & Blakely, R.D. Neurotoxin-induced degeneration of dopamine neurons in *Caenorhabditis elegans*. *Proc. Natl. Acad. Sci. USA* **99**, 3264–3269 (2002).